Supplement of Atmos. Meas. Tech., 11, 3351–3372, 2018
https://doi.org/10.5194/amt-11-3351-2018-supplement

Atmospheric Measurement Techniques
Open Access

Supplement of

Dynamic–gravimetric preparation of metrologically traceable primary calibration standards for halogenated greenhouse gases

Myriam Guillevic et al.

Correspondence to: Myriam Guillevic (myriam.guillevic@metas.ch)

S1 Determination of mass loss rate of permeation devices

The mass loss q_m in ng/min due to permeation through the membrane of the permeation device is calculated using a linear fit based on multiple data of mass and time as measured by our magnetic suspension balance. This linear fit gives directly q_m and the associated standard deviation used in the uncertainty budget as $Stab_{balance}$. However, to calculate the expanded uncertainty of the mass loss it is needed to take into account the reading resolution of the balance. To include this in the uncertainty we decompose q_m into the first data point (m_1, t_1) and the final data point (m_2, t_2). (m_1, t_1) is directly taken as the first data from the set used to calculate the linear fit. t_2 is taken from the last data point of the set. m_2 is re-calculated using the values of m_1, t_1, t_2 and q_m so that is it consistent:

$$m_2 = m_1 - q_m \cdot (t_2 - t_1)$$

It is now possible to associate to each variable m_1, m_2, t_1 and t_2 the uncertainty of the reading resolution (respectively 0.0000005 g and 0.05 s, as reported in Table 2 of the main text).

S2 Cryo-filling: dead volume correction

When filling a cylinder, at the end of the filling routine the nitrogen gas present in between the pneumatic valve V1 and the valve of the cylinder is lost. This is due to the saturation vapour pressure of nitrogen in equilibrium with the liquid nitrogen. This pressure is a function of liquid nitrogen temperature. Before doing any of the filling, we therefore determined how much gas is exactly lost, by measuring the residual pressure in this volume when the cylinder is filled with some air and placed in the filled liquid nitrogen bath.

For this test, the pressure gauge was placed directly in between the cylinder and V1. Synthetic air was filled in the cylinder placed in liquid nitrogen, V1 was closed, and the pressure was measured in this closed system. The pressure was at 800 hPa, in agreement with a liquid nitrogen temperature of $-$ 200 °C.

To compensate for this loss, before switching valves V1 and V2 to start filling the cylinder, the interval in between V1 and the cylinder valve is flushed with the carrier gas three times and then filled at 800 hPa. This volume of gas is then trapped in the cylinder when the valves are switched at the beginning of the filling. This volume compensates for the approximately equivalent volume lost at the end.

S3 Weighted linear fit: York algorithm

To calculate the weighted linear fit taking into account the standard uncertainties $u_{R_{prep,i,j}}$ and $u_{R_{meas,i,j}}$ of both $R_{prep,i,j}$ and $R_{meas,i,j}$, we apply the York algorithm (York et al., 2004) as written in Cantrell (2008). $u_{R_{prep,i,j}}$ are calculated according to Equ. 8 in the main text. $u_{R_{meas,i,j}}$ are the standard deviation of the mean of $R_{meas,i,j}$ and documented in Table S5.

First, input values are initialised. For a given substance j, and with i representing all accepted cylinder values (i.e. all values except outliers), we set:

$$x_i = R_{prep,i,j}$$

$$y_i = R_{meas,i,j}$$

$$w_{x_i} = (1/u^2_{R_{prep,i,j}})$$

$$w_{y_i} = (1/u^2_{R_{meas,i,j}})$$

$$a = 1$$

$$r_i = 0$$

$$\alpha_i = \sqrt{w_{x_i} \cdot w_{y_i}}$$

The following algorithm is then ran 10 times:

$$W_i = \frac{w_{x_i} \cdot w_{y_i}}{w_{x_i} + a^2 \cdot w_{y_i} - 2 \cdot a \cdot r_i \cdot \alpha_i}$$

$$\bar{x} = \frac{\sum W_i \cdot x_i}{\sum W_i}$$

$$\bar{y} = \frac{\sum W_i \cdot y_i}{\sum W_i}$$

$$U_i = x_i - \bar{x}$$

$$V_i = y_i - \bar{y}$$

$$B_i = W_i \cdot \left(\frac{U_i}{w_{y_i}} + \frac{a \cdot V_i}{w_{x_i}} - (a \cdot Ui + Vi) \cdot \frac{r_i}{\alpha_i} \right)$$

$$a = \frac{\sum Wi \cdot Bi \cdot Vi}{\sum Wi \cdot Bi \cdot Ui}$$

After these ten runs (which are in this case more than necessary to reach convergence of a), the final value for b is computed:

$$b = \bar{y} - a \cdot \bar{x}$$

The standard uncertainty (k = 1) for the obtained parameters is calculated as follow:

$$\bar{B} = \frac{\sum W_i \cdot B_i}{\sum W_i}$$

$$\sigma_a = \sqrt{\frac{1}{\sum Wi \cdot (Bi - \bar{B})^2}} \cdot \frac{1}{\sqrt{length(x_i)}}$$

$$\sigma_b = \sqrt{\frac{1}{\sum Wi} + (\bar{x} + \bar{B})^2 \cdot \sigma_a^2} \cdot \frac{1}{\sqrt{length(x_i)}}$$

S4 METAS-2015 scales for HFC-125 and HFO-1234yf

Diagrams presenting the experimental setup used to prepare reference gas mixtures for HFC-125 and HFO-1234yf are presented in Fig. S2 (permeation and cryo-filling) and Fig. S3 (additional dynamic dilution).

The main technical differences with the METAS-2017 preparation method are:

- the carrier gas is additionally purified at the beginning of the preparation, using a commercially available purification cartridge (Microtorr, SAES Getters).
- only one dilution step is used after the permeation chamber (MFC1, MFC2);
- only one cryo-filling routine is done for each cylinder (there are no multiple fillings). As a result each cylinder contains a reference gas mixture for only one substance.
- the reference gas mixture in the produced cylinder is at nmol/mol (ppb) level and therefore needs additional dilution. This is done dynamically using a setup called 'METAS 2-step-dilutor' already existing at METAS, based on two successive dynamic dilution steps (Fig. S3).
- the mixture exiting the '2-step-dilutor' is directly injected into the Medusa-GC-MS system in operation at Empa for measurement.

S5 Measurement of impurities in the permeation device for HFC-125

Based on the findings from Vollmer et al. (2015) who identified several potential impurities in HFC-125 inherited from its production pathway, we have measured the presence of impurities in the permeator for HFC-125. We have done this test using the reference gas mixture for HFC-125 prepared at 85 nmol/mol (cylinder MP15-4020, see Fig. S1) as part of the METAS-2015 suite for HFC-125. These measurements have been performed by injecting 1 L of this mixture directly in the Medusa-GC-MS at Empa. The detection of the HFC-125 peak was disabled to avoid saturation of the detector. For HCFC-132b, there was no chromatographic baseline excursion suggesting that the mole fraction was well below the detection limit (defined here as three times the noise level). As the amount of gas used for a measurement was 1 L, i.e. half the normal gas quantity of 2 L, we roughly estimate the detection limit for HCFC-132b as twice the detection limit for a normal measurement of 2 L, i.e. 0.03 pmol/mol (instead of 0.015 pmol/mol).

In addition, the measurements showed the presence of:

– CFC-115: 31 pmol/mol ($0.36 \cdot 10^{-3}$ mol per mol HFC-125)

– HFC-143a: 51 pmol/mol ($0.6 \cdot 10^{-3}$ mol per mol HFC-125)

– HFC-134a: 31 pmol/mol ($0.36 \cdot 10^{-3}$ mol per mol HFC-125)

– HCFC-124: 11 pmol/mol ($0.13 \cdot 10^{-3}$ mol per mol HFC-125)

– SF_6: 0.2 pmol/mol with LOD = 0.03 pmol/mol ($2.5 \cdot 10^{-6}$ mol per mol HFC-125)

– HFO-1234yf: 0.06 pmol/mol with LOD = 0.02 pmol/mol, although we are not sure if this is a small impurity introduced potentially by contamination from a regulator

– CFC-13: no baseline disruption (LOD = 0.14 pmol/mol).

In cylinder MP-001 containing 32.027 pmol/mol HFC-125, the SF_6 impurities originating from the HFC-125 permeator correspond to a contribution of $2.5 \cdot 10^{-6} \cdot 32.027 = 0.00008$ pmol/mol SF_6. This can be neglected compared to the prepared 10.582 pmol/mol SF_6. The same conclusion applies to HFO-1234yf and to the other cylinders.

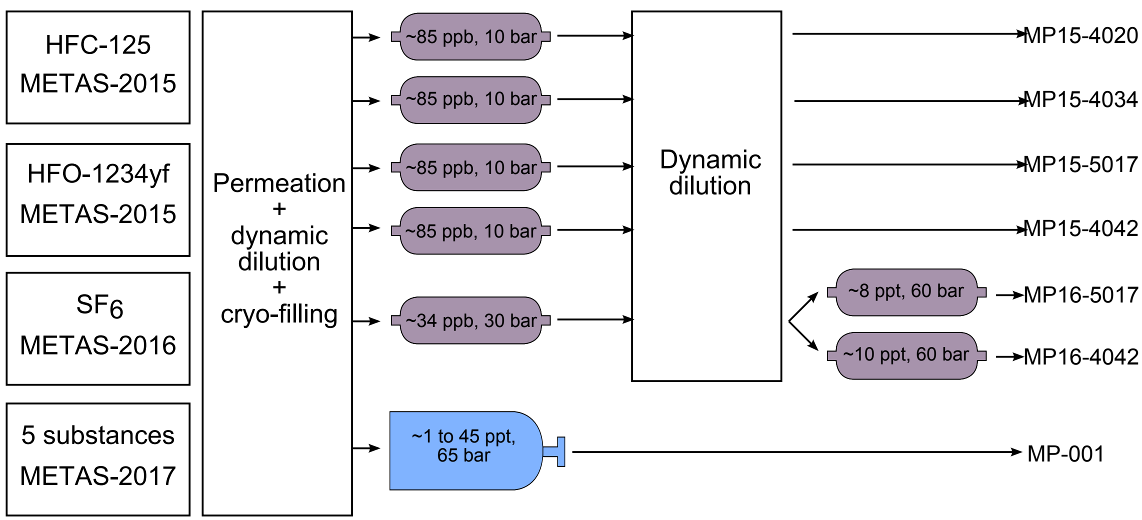

Figure S1. Overview of preparation steps for the 3 successive generations of scales prepared at METAS: METAS-2015, METAS-2016 and METAS-2017. The METAS-2017 scale is the most advanced scale in terms of minimisation of exposition to metal surfaces. ppb: nmol/mol. ppt: pmol/mol.

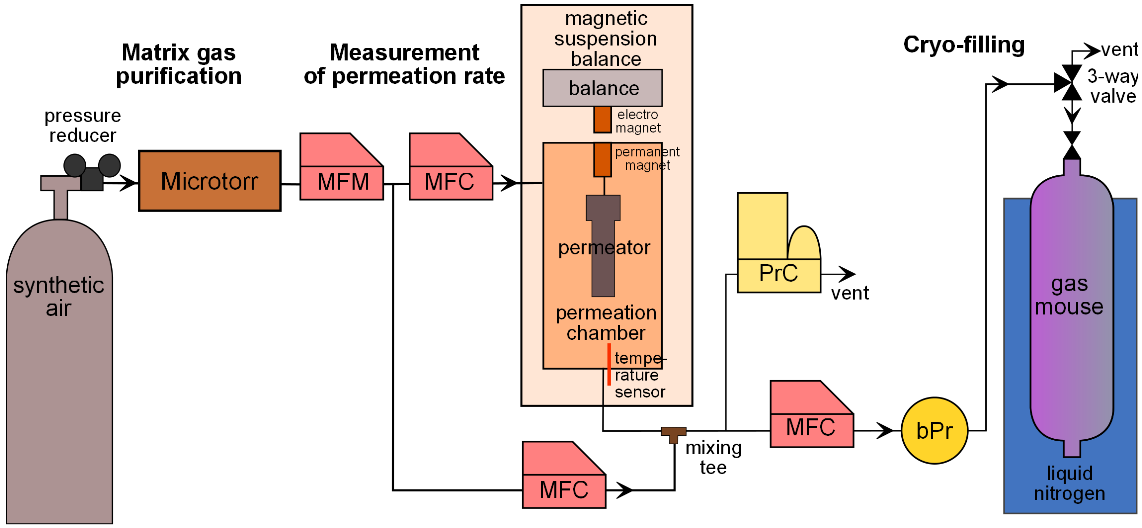

Figure S2. Preparation setup used to produce high concentration mixtures for HFC-125 and HFO-1234yf in cylinders.

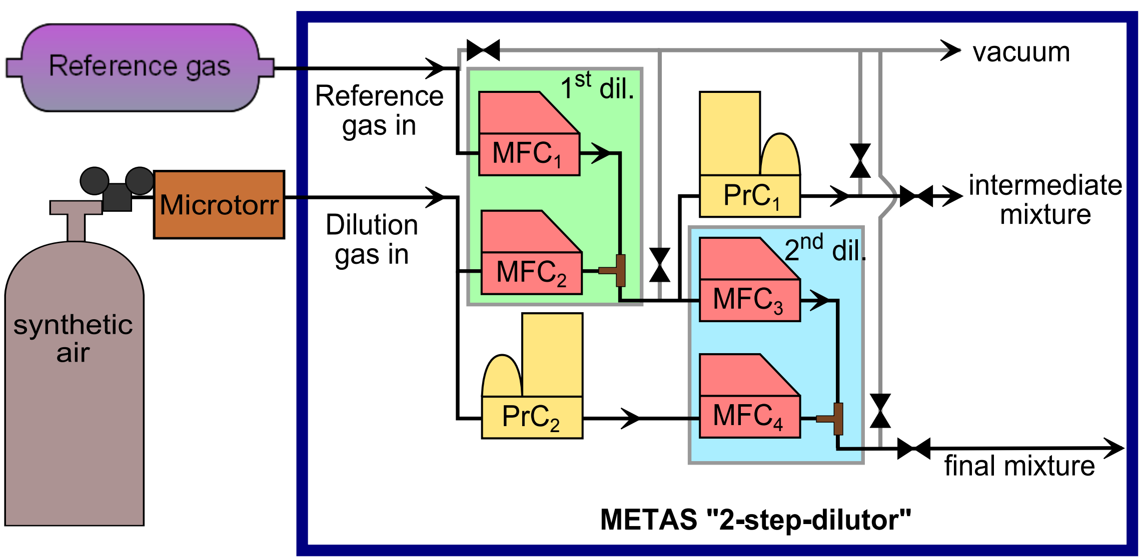

Figure S3. Schematic of METAS '2-step-dilutor', a two-stage dynamic dilutor based on thermal mass flow controllers. This setup is used to dilute the high concentration cylinders for HFC-125, HFO-1234yf and SF_6 (see preparation overview in Fig. S1). The final mixtures are at pmol/mol levels.

Table S1. Mass loss rate determination for each permation device.

	m_1, g	m_2, g	t_1, min	t_2, min	q_m, ng/min	$Stab_{balance}$, % (k = 1)
SF_6	28.44957646	28.43612094	5999.45	14130.80	1654.77	0.20
HFC-125	28.56911448	28.56634188	1505.17	7128.32	493.07	0.40
HFO-1234yf	30.40242526	30.39984672	998.70	30205.77	88.28	0.41
HCFC-132b	29.46146154	29.46037128	89.83	10068.25	109.26	0.64
CFC-13	30.09772063	30.09634635	5999.55	12319.95	217.44	0.57

Table S2. Flows used for the first and second dynamic dilution steps, in mL/min @ STP. MFM measures the total flow MFC1 + MFC2. MFC1 and MFC2 therefore do not need individual calibration.

	MFC1	MFC2	MFM	MFC3	MFC4
Set points					
SF_6	167	4500	-	10	5000
HFC-125	167	500	-	10	4000
HFO-1234yf	167	3500	-	10	4000
HCFC-132b	300	3500	-	10	4000
CFC-13	300	3000	-	10	4000
water vapour	300	1200	-	not used	not used
Calibrated values					
SF_6	-	-	4594.968	10.809	5115.463
HFC-125	-	-	676.333	10.809	4109.936
HFO-1234yf	-	-	3691.690	10.809	4109.936
HCFC-132b	-	-	3817.535	10.809	4109.936
CFC-13	-	-	3333.618	10.809	4109.936
water vapour	-	-	not calibrated	not used	not used

Table S3. Filling durations, in seconds.

Cylinder	MP-001	MP-002	MP-003	MP-004	MP-005	MP-006	MP-007	MP-008	MP-009	MP-010	MP-011
SF_6	4018	2040	1546	1546	1915	1178	1178	1166	1296	1060	1190
HFC-125	4018	2040	1546	1546	1915	1178	1178	1166	1296	1060	1190
HFO-1234yf	4018	2040	1546	1546	1915	1178	1178	1166	1296	1060	0
HCFC-132b	4018	2040	1546	1546	1915	1178	1178	1166	1296	1060	1190
CFC-13	4018	2040	1546	1546	1915	1178	1178	1166	1296	1060	1190
water vapour	24110	10200	8470	8470	6625	10310	7070	7130	6480	7660	8200

Table S4. Matrix gas impurity content: results of measurement by Medusa-GC-MS (molar fraction, pmol/mol). For the uncertainty budget we use a triangular distribution centered in this measured molar fraction, with the same value as half width of limit.

	SF_6	HFC-125	HFO-1234yf	HCFC-132b	CFC-13
Molar fraction, pmol/mol	0.006	0.04	0.003	0.003	0.015
Half width of limit, pmol/mol	0.006	0.04	0.003	0.003	0.015

Table S5. Results of measured ratios without correction of analyser response. n is the number of replicate measurements. For cylinder MP-001, by default the ratio is set to 1, and we apply as standard deviation the average standard deviation over the set of cylinders, for each given substance. $u_{R_{meas}}$ is the standard deviation of the mean.

Cylinder	MP-006	MP-010	MP-008	MP-001	MP-007	MP-011	MP-003	MP-004	MP-002	MP-009	MP-005
					SF_6						
R_{meas}	0.800	0.898	0.971	1.000	0.998	1.008	1.052	1.052	1.106	1.102	1.308
n	20	9	19	12	9	10	9	10	18	10	12
$u_{R_{meas}}$	0.001	0.001	0.001	0.001	0.001	0.001	0.001	0.001	0.001	0.001	0.001
					HFC-125						
R_{meas}	0.804	0.905	0.978	1.000	1.004	1.015	1.049	1.051	1.120	1.111	1.308
n	20	10	17	12	9	9	10	10	18	10	12
$u_{R_{meas}}$	0.001	0.001	0.001	0.001	0.001	0.001	0.001	0.001	0.001	0.001	0.002
					HFO-1234yf						
R_{meas}	0.799	0.846	0.931	1.000	0.995	-	1.062	1.051	1.086	1.076	1.305
n	20	9	18	11	9	-	10	10	19	10	12
$u_{R_{meas}}$	0.003	0.002	0.003	0.003	0.003	-	0.004	0.004	0.004	0.004	0.006
					HCFC-132b						
R_{meas}	0.799	0.881	0.979	1.000	1.002	1.010	1.079	1.049	1.094	1.096	1.300
n	19	9	18	12	9	10	10	10	19	10	12
$u_{R_{meas}}$	0.001	0.002	0.002	0.002	0.002	0.002	0.002	0.002	0.002	0.002	0.002
					CFC-13						
R_{meas}	0.786	0.890	0.979	1.000	0.988	0.997	1.042	1.054	1.103	1.088	1.294
n	20	8	19	12	9	8	9	9	19	10	12
$u_{R_{meas}}$	0.004	0.002	0.005	0.004	0.006	0.003	0.003	0.003	0.005	0.006	0.006

Table S6. Measured & corrected ratios using a linear fit.

Cylinder	MP-006	MP-010	MP-008	MP-001	MP-007	MP-011	MP-003	MP-004	MP-002	MP-009	MP-005
R_{prep}	0.800	0.900	0.990	1.000	1.000	1.010	1.050	1.050	1.100	1.100	1.300
U	0.002	0.003	0.003	0.003	0.003	0.003	0.003	0.003	0.003	0.003	0.004
U, %	0.3	0.3	0.3	0.3	0.3	0.3	0.3	0.3	0.3	0.3	0.3
SF_6											
$R_{meas,corr}$	0.804	0.899	0.971	0.999	0.998	1.007	1.051	1.050	1.103	1.099	1.301
U	0.007	0.008	0.008	0.008	0.009	0.009	0.009	0.009	0.009	0.009	0.011
U, %	0.9	0.9	0.9	0.8	0.9	0.8	0.8	0.8	0.8	0.8	0.8
HFC-125											
$R_{meas,corr}$	0.802	0.901	0.974	0.996	1.000	1.011	1.044	1.045	1.114	1.106	1.300
U	0.007	0.008	0.009	0.009	0.009	0.009	0.009	0.009	0.010	0.010	0.011
U, %	0.9	0.9	0.9	0.9	0.9	0.9	0.9	0.9	0.9	0.9	0.9
HFO-1234yf											
$R_{meas,corr}$	0.807	0.854	0.937	1.005	0.999	NaN	1.065	1.054	1.089	1.080	1.305
U	0.014	0.014	0.015	0.016	0.016	NaN	0.017	0.017	0.017	0.017	0.021
U, %	1.7	1.7	1.6	1.6	1.6	NaN	1.6	1.6	1.6	1.6	1.6
HCFC-132b											
$R_{meas,corr}$	0.800	0.883	0.981	1.001	1.004	1.012	1.080	1.050	1.095	1.097	1.301
U	0.011	0.011	0.012	0.013	0.013	0.013	0.014	0.013	0.014	0.014	0.016
U, %	1.3	1.3	1.3	1.3	1.3	1.3	1.3	1.3	1.3	1.3	1.2
CFC-13											
$R_{meas,corr}$	0.799	0.901	0.988	1.009	0.997	1.006	1.050	1.062	1.109	1.095	1.297
U	0.014	0.014	0.016	0.016	0.017	0.016	0.017	0.017	0.018	0.018	0.021
U, %	1.7	1.6	1.7	1.6	1.7	1.6	1.6	1.6	1.6	1.6	1.6

References

Cantrell, C. A.: Technical Note: Review of methods for linear least-squares fitting of data and application to atmospheric chemistry problems, Atmos. Chem. Phys., 8, 5477–5487, https://doi.org/10.5194/acp-8-5477-2008, 2008.

Vollmer, M. K., Reimann, S., Hill, M., and Brunner, D.: First observations of the fourth generation synthetic halocarbons HFC-1234yf, HFC-1234ze(E), and HCFC-1233zd(E) in the atmosphere, Environ. Sci. Technol., 49, 2703–2708, https://doi.org/10.1021/es505123x, 2015.

York, D., Evensen, N. M., Martínez, M. L., and Delgado, J. D. B.: Unified equations for the slope, intercept, and standard errors of the best straight line, Am. J. Phys., 72, 367–375, https://doi.org/10.1119/1.1632486, 2004.